Proceedings of IMECE
International Mechanical Engineering Congress and Exposition
November 5-10, 2000. Orlando, Florida.

DESIGN OF A BIOMIMETIC DIRECTIONAL MICROPHONE DIAPHRAGM

C. Gibbons and R. N. Miles

Department of Mechanical Engineering
State University of New York

Binghamton, NY 13902-6000

ABSTRACT

A miniature silicon condenser microphone diaphragm has been designed that exhibits good predicted directionality, sensitivity, and reliability. The design was based on the structure of a fly's ear (*Ormia ochracea*) that has highly directional hearing through mechanical coupling of the eardrums. The diaphragm that is 1mm x 2mm x 20 microns is intended to be fabricated out of polysilicon through microelectromechanical micromachining. It was designed through the finite-element method in ANSYS in order to build the necessary mode shapes and frequencies into the mechanical behavior of the design. Through postprocessing of the ANSYS data, the diaphragm's response to an arbitrary sound source, sensitivity, robustness, and Articulation Index - Directivity Index (AI-DI) were predicted. The design should yield a sensitivity as high as 100 mV/Pa, an AI-DI of 4.764 with Directivity Index as high as 6 between 1.5 and 5 kHz. The diaphragm structure was predicted be able to withstand a sound pressure level of 151.74 dB. The sound level that would result in collapse of the capacitive sensor is 129.9 dB.. The equivalent sound level due to the self-noise of the microphone is predicted to be 30.8 dBA.

INTRODUCTION

Silicon microfabrication technology shows significant potential for enabling the development of novel sensors for sound and vibration. Many of the recent efforts at employing this technology for microphone design have focussed on the fabrication of small, non-directional microphone diaphragms made of silicon and incorporating capacitive sensing [1,2,3]. Often these small microphones have been paired together to create a directional microphone, but have experienced performance problems with this method [4,5,6]. While silicon technology has potential advantages over previous methods of fabricating existing microphone designs, it also provides the possibility of realizing radically new design concepts. In the present study, we present a design of a miniature silicon microphone diaphragm that takes advantage of the ability to fabricate complicated, patterned membranes to achieve directional acoustic response.

The directional microphone design described here is inspired by our previous efforts at understanding the mechanics of directional hearing in small animals such as insects. Many small animals depend on the ability to localize sound sources either for predator avoidance or mate selection. All animals having two tympanal ears localize sound by processing interaural differences either in the time of arrival or level of the acoustic pressure. When the size of the animal is very small relative to the sound wavelength, these interaural differences can be too small to permit accurate processing by the central nervous system to allow sound source localization. Certain small animals that depend on localizing sound sources have evolved either air-borne or structure-borne connections between the tympanal membranes, or eardrums. By suitable coupling of the motions of the tympana, it is possible for each to respond preferentially to sound from certain directions. Our analysis of the coupled ears of the parasitoid fly, *Ormia ochracea*, (Order: Diptera, Family: Tachinidae, subfamily: ormiine) has inspired a novel approach to constructing small, directional sound receivers [7-10].

The mechanically coupled ears of *Ormia ochracea* have been shown to respond predominantly in two resonant modes of vibration, one in which both tympana move in opposite directions and one in which they both move in-phase [7]. With

the proper set of mechanical parameters, this pair of modes in an acoustic receiver can provide the proper combination of the acoustic pressure gradient and the pressure so that each membrane has a cardioid directivity pattern [8,11]. To achieve this directional response, the pressure sensing membranes must be designed carefully to reduce the influence of unwanted vibrational modes. The main goal of the present study is to describe a candidate microphone diaphragm design that mimics the mechanically coupled ears of *Ormia ochracea*.

Since the pair of ears of *Ormia ochracea* are only about 1mm across, the design concept for a directional microphone examined here clearly has potential for providing directionality in a very small microphone package. Our current goal is to develop a directional microphone diaphragm design that is suitable for small packages such as in-the-ear hearing aids. There is significant interest in incorporating directional microphones in hearing aids because it improves speech intelligibility in noisy environments.

NOMENCLATURE

Corrugated diaphragm, capacitive directional microphone, micromachining (MEMS), finite element analysis, Articulation Index, Directivity Index.

1.Microphone Design

The diaphragm design described in the following is intended to be fabricated through MEMS technology, and therefore polysilicon is an appropriate material to use [12,13]. The material properties used in all analyses and calculations are modulus of elasticity, 170 GPa, density, 2300 kg/m^3, Poisson's ratios, 0.3, and yield stress, 1.7 GPa. The overall size of the diaphragm is 1mm x 2 mm x 20 microns wide, with a poly film thickness of 0.25 microns.

The diaphragm design makes use of corrugations to decrease fabrication stress as well as increase sensitivity [14-18]. It also utilizes solid stiffeners and bosses to create the necessary local stiffness to create the two main modes of movement [19]. All of the sharp corners of the design have been filleted to help further reduce stress concentrations [18]. Figure 1 displays the model in an oblique view.

The diaphragm is intended for use in a capacitive sensing microphone, which requires a perforated backplate a small gap distance away, a large air cavity, and an air vent to counteract the fluctuations in the atmospheric pressure [20,21]. For the calculations, the air gap between the diaphragm and backplate is assumed to be 3 microns.

For the FEM model, element type shell63 (three-dimensional quadrilateral shell, 6 dof's per node) was used for the membrane structure of the diaphragm, and solid45 (8 node brick) was used for the solid stiffeners and bosses. To model the appropriate boundary conditions, all of the nodes along the boundary of the diaphragm have their degrees of freedom set to zero to simulate the fully clamped boundaries [22,23]. The model contains of a total of 10,683 nodes and 10,144 elements.

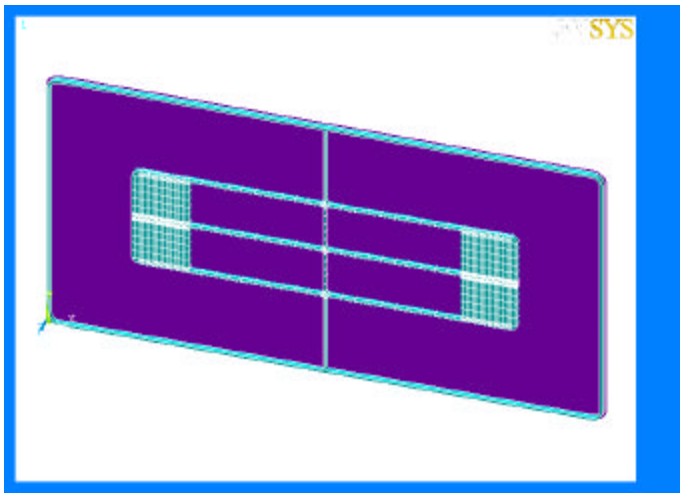

Fig. 1. Diaphragm model.

2. Analyses

2.1 Modal

The full model has been used in the analysis and the subspace method has been used for extracting the resonant frequencies and mode shapes. The two resonant frequencies are 1272 and 9349 Hz, and their corresponding mode shapes are shown in Fig. 2 and 3 respectively.

The mode shape data shown in figures 2 and 3 were saved and processed using FORTRAN in order to create the modal matrix, *[U]*, for use in calculating the response to sound that is incident from any direction.

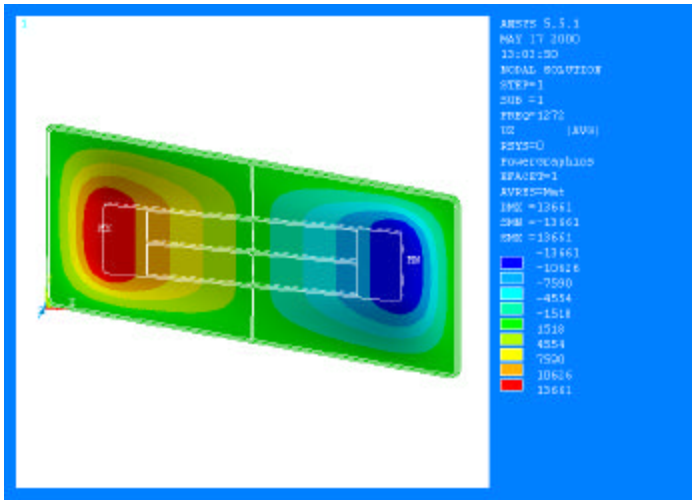

Fig. 2. Mode shape 1. Rocking, out-of-phase mode.

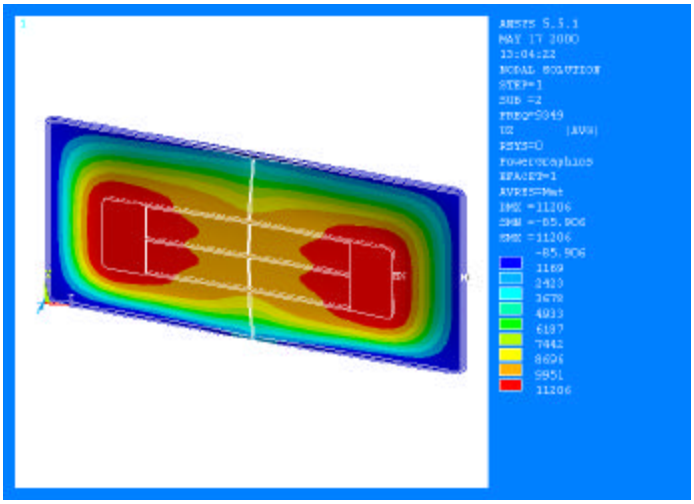

Fig. 3. Mode shape 2. Symmetric, in-phase mode.

3.2 Pressure

In order to obtain an estimate of the microphone diaphragm sensitivity and an estimate of the maximum sound pressure the diaphragm can endure, a static analysis was performed of the displacement resulting from a 1 Pa pressure load. The 1 Pa static pressure was applied to the bottom level areas of the diaphragm in the negative *z* direction. After solving for the response to a uniform static pressure, the maximum stress encountered was used to calculate the maximum sound pressure load that the diaphragm should be able to handle. The model shows a maximum stress of 2.2 MPa due to this 1 Pa loading. Relating this stress resulting from a unit pressure to the yield stress of the material will approximate the maximum static pressure allowable. The root mean square pressure, $P_{rms}^{\ 2}$, is then:

$$P_{rms}^{\ 2} = \frac{1}{T}\int_0^T P^2(t)dt = P_{\max}^{\ 2} \qquad (1)$$

because this was a static approach. Then the maximum sound pressure level is:

$$SPL(dB) = 10\log_{10}\left(\frac{P_{rms}^{\ 2}}{P_{ref}^{\ 2}}\right) = 10\log_{10}\left(\frac{P_{\max}^{\ 2}}{P_{ref}^{\ 2}}\right), \qquad (2)$$

where $P_{ref}^{\ 2}$ is 20 E-6 Pa. Based on this, the diaphragm structure was estimated to be able to withstand a sound pressure level of 151.74 dB. Note that the actual maximum SPL the microphone can endure will also depend on the bias voltage and air gap between the diaphragm and backplate.

An estimation for the maximum SPL that the microphones would be able to withstand can be found through the use of the microphone collapse criteria. It is well known that the force due to the voltage between the diaphragm and backplate can result in a collapse of the diaphragm against the backplate if the diaphragm deflection approaches 2/3 of the nominal gap distance, *d* [20]. Given the mechanical sensitivity of the diaphragm, an estimation for the SPL that would result in a failure of the microphone can be found. The mechanical sensitivity can be represented by the displacement of the bosses under the 1 Pa load. The mechanical sensitivity is:

$$S_m = \frac{d}{1Pa}, \qquad (3)$$

where *d* is the displacement [22]. The mechanical sensitivity was found to be 0.032 microns/Pa. The approximate collapse SPL is then:

$$SPL_{collapse} = 20\log_{10}\left(\frac{2d}{3P_{ref}S_m}\right), \qquad (4)$$

where *d* is the air gap distance between the diaphragm and backplate. The estimated $SPL_{collapse}$ was found to be 129.9 dB.

The minimum detectable signal of the diaphragm depends on the viscous damping in the design [24]. The damping constant of the model was found by:

$$[C] = [U]^{T^{-1}}\left[\ddots\ 2w_i x_{i\cdot}\ddots\right][U]^{-1},\ \text{i=1,2} \qquad (5)$$

where *[U]* is the modal matrix of the model. The minimum detectable signal for this design was found to be 30.8 dBA.

A quick approximation of the diaphragm's sensitivity can be found through the combination of its mechanical and electrical sensitivities. The electrical sensitivity is:

$$S_e = \frac{V_b}{d}, \qquad (6)$$

where V_b is the bias voltage and again *d* is the air gap [25]. For the calculations, a V_b of 10 volts and a *d* of 3 microns were assumed. The total sensitivity is then:

$$S = S_e S_m. \qquad (7)$$

From this simple calculation, the sensitivity of the model is found to be approximately 106.7 mV/Pa. This is found to be in reasonable agreement with the results of more detailed calculations described in the following.

For the force vector calculations, each node needed to have a force assigned to it. To do this most accurately, the results from the pressure analysis in ANSYS were used. An element table was formed in the postprocessor, which displayed the force assigned to each element of the model. A list of all of the elements and their corresponding nodes was acquired. The element force was then multiplied by a factor of 1/3 or ¼ depending on whether it was a three or four node element. This force was then assigned to the all of the nodes of the element and was added to any contributions from neighboring elements. This ensured the correct nodal force in the z direction for all of the nodes of the model. These were then used as the amplitude of the force on each node as will be discussed in the next section.

3. Response Calculations

3.1 Force Vector

The force from a plane sound wave can be calculated as follows:

$$f_i = amp_i \exp(-ik_x x_i)\exp(-ik_y y_i)\exp(-ik_z z_i), \quad (8)$$

where amp_i is the nodal force amplitude, x_i, y_i, z_i are the node coordinates and

$$k_x = \left(\frac{w}{c}\right)\cos(q), \quad (9)$$

$$k_y = \left(\frac{w}{c}\right)\sin(q)\sin(f), \quad (10)$$

$$k_z = \left(\frac{w}{c}\right)\sin(q)\cos(f). \quad (11)$$

Here ω is the frequency of the sound source, c is the speed of sound, and the angles are as follows:

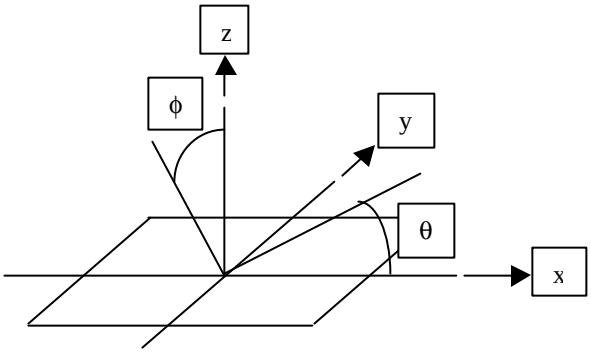

Fig. 4. Coordinate system of the diaphragm.

Now a forcing vector can be created for any sound source incident at any angle.

3.2 Classic Modal Approach

With the modal file and forcing vector, the model's response was calculated with the classic modal analysis. The modal forces, $\underline{q}$, are:

$$\underline{q} = [U]^T \underline{f}, \quad (12)$$

where $[U]^T$ is the transpose of the modal matrix that was built earlier and $\underline{f}$ is the forcing vector. The modal coordinates, $\underline{\eta}$, and physical coordinates, $\underline{z}$, were then calculated by

$$h_j = \frac{q_j}{w_j^2 - w^2 + 2wx_j w_j i}, \text{ j=1,2} \quad (13)$$

$$\underline{z} = [U]\underline{h}, \quad (14)$$

where the w_j for j=1,2 are the two natural frequencies and x_j are the two corresponding damping ratios. The physical coordinate vector is complex, so it is useful to calculate the response phase and magnitude in dB:

$$\underline{magnitude} = 20\log_{10}|\underline{z}|, \quad (15)$$

$$\underline{phase} = \tan^{-1}\left(\frac{imag(\underline{z})}{real(\underline{z})}\right). \quad (16)$$

The above calculations give results for assumed damping ratios for each of the two natural frequencies. It is important to find the two damping ratios that yield the best response possible from the design. For this, a Matlab GUI was created that utilized slider bars to vary the ratios, and produce immediate plots of the response of the two best representative nodes of the diaphragm. These nodes were located centrally and symmetrically along the x-axis and could be found on the outer most edge of the left and right bosses. It was found that for this design, damping ratios of 0.1 and 9.0 yielded the best results for the AI-DI for the first and second resonant modes respectively. It was assumed that the damping would be created by the airflow along the air gap and through the backplate's holes. The results are presented with units of sensitivity, in mV/Pa, so the plots displaying the model's overall sensitivity versus frequency. The following plot is an example of the diaphragm's response (sensitivity) for the two above mentioned damping ratios as shown in the GUI:

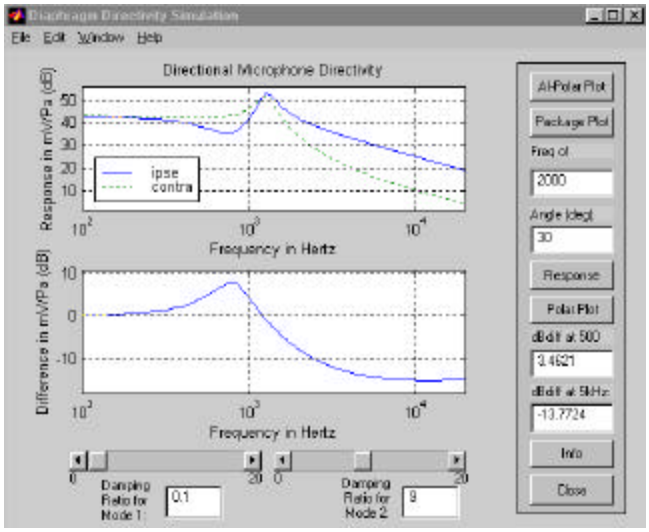

Fig. 5. Diaphragm response versus frequency.

It can be seen from figure 5 that the model's sensitivity in decibels is about 40 (dB Re 1mV/Pa), which is equivalent to 100 mV/Pa. This result correlates well with the previous sensitivity hand calculation.

The GUI also includes buttons that produce calculations and plots for Directivity Index versus frequency, AI-DI polar plots, polar plots and an animated response of the diaphragm for a specific frequency and incident angle, q. Lastly, a button is included that produces an AI-DI polar plot (as described below) of the completed microphone with packaging

in place. The following figure is an example of the polar plot of the diaphragm at 5000 Hz:

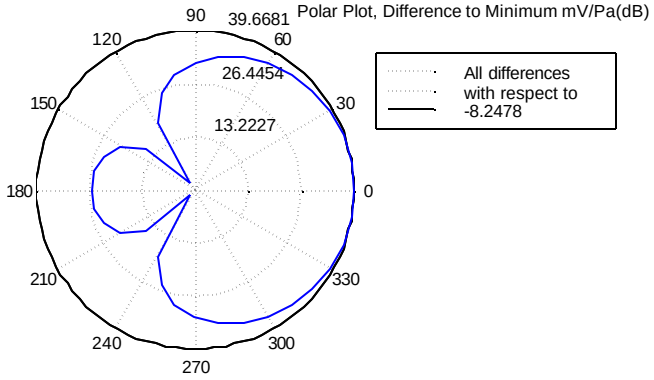

Fig. 6. Polar plot of design at 5000 Hz.

3.3 Directivity Index and AI-DI

The Directivity Index approximates a microphone's directivity for a certain frequency [26]. When combined with the Articulation Index, a representative number for the overall directivity of the microphone for all frequencies can be obtained. The DI is based on the ratio of the response of incidence excitation (θ and ϕ equal 0) to the average of the microphone's response for all other angles of theta. The equations are as follows:

$$DI = 10\log_{10} Q, \tag{17}$$

where Q is the Directivity Factor:

$$Q = \frac{e^2(0,0,w)}{\langle e^2 \rangle}. \tag{18}$$

e is the response of the microphone for a certain angle and frequency, $e(q,f,w)$. $e(0,0,w)$ is the response of the incident side of the diaphragm, and $\langle e^2 \rangle$ is the average of the response for all values of q, with f set to zero [27]. To get the Articulation Index – Directivity Index, the AI is applied to the DI in a form of a weighting factor for the particular frequency [28,29]. There are many methods for applying an AI weighting, such as the popular 14-band method:

Frequency (Hz)	A-I Weighting
250	.03
315	.03
400	.04
500	.04
630	.06
800	.06
1000	.08
1250	.09
1600	.11
2000	.11
2500	.11
3150	.11
4000	.07
5000	.06

Fig. 7. AI weightings and frequencies [30].

The following two plots display the DI versus frequency and the AI-DI polar plot for the design.

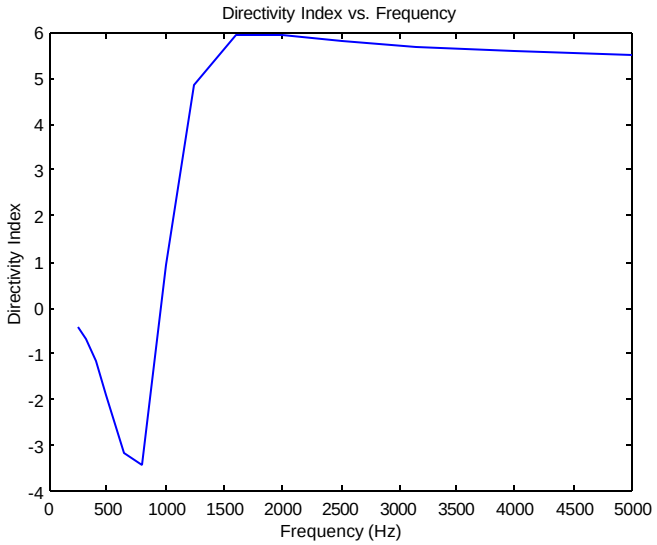

Fig. 8. Directivity Index versus the 14 frequencies.

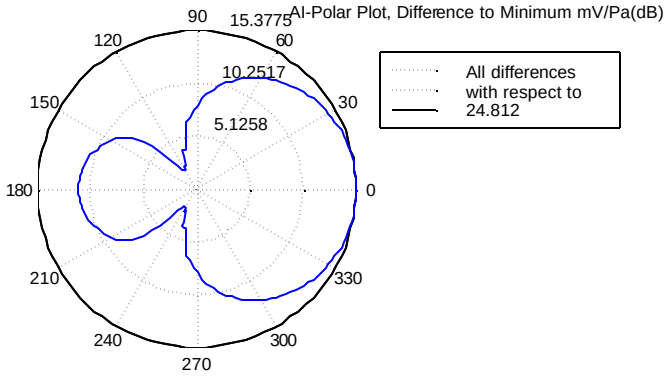

Fig. 9. AI-DI polar plot.

Fig. 8 shows that the design displayed good directivity between 1500 and 5000 Hz.

3.4 Package Estimation

Calculations have also made to estimate the behavior of the diaphragm after the microphone packaging is in place. It is assumed that the package consists of two small closely placed holes, one over each side of the diaphragm. This package effects how the sound waves encounter the diaphragm. It is assumed that the sound waves will be incident as plane waves, with a time lag between the two sides. In order to

complete the desired calculations, a new forcing vector is needed:

$$f_i = amp_i \exp(iwt), \quad (19)$$

for the side of the diaphragm that is closest to the sound source, and

$$f_i = amp_i \exp(-iwt), \quad (20)$$

for the opposite side. Again amp_i is the nodal force amplitude and t is the time lag:

$$t = \frac{L}{2c}\cos(q), \quad (21)$$

where c is the speed of sound, and L is the distance between the two holes of the packaging. The results from these calculations show that the packaging will not destroy the directional sensitivity of the diaphragm.

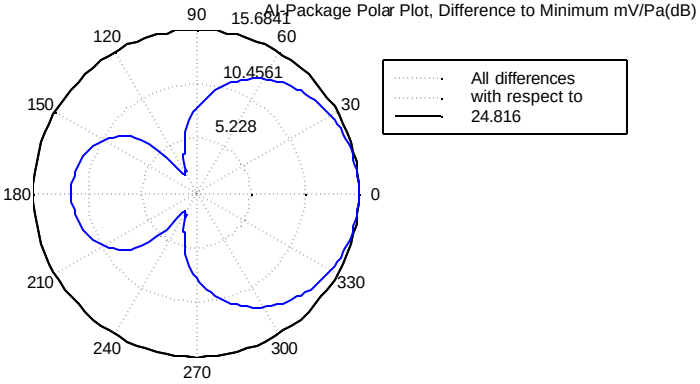

Fig. 10. AI-DI of model with hearing aid packaging in place.

4. Conclusion

Based on the structure of the auditory system of the fly *Ormia ochracea*, a directional microphone diaphragm has been designed and its behavior has been predicted. It was designed through FEM analysis and the results from the program were used to calculate the diaphragm's response to an arbitrary sound source found anywhere in space. The results for the design were quite good, yielding decent AI-DI, sensitivity, robustness and overall response.

ACKNOWLEDGMENTS

This work has been supported by the National Institutes of Health, grant number 1 R01 DC03926-01 to RNM.

REFERENCES

[1] G.M. Sessler, New Acoustic Sensors, Journal De Physique IV, 2 (1992) 413-419

[2] G.M. Sessler, Silicon Microphones, Journal of Audio Engineering Society, 44, ½ (1996) 16-22

[3] G.M. Sessler, Acoustic Sensors, Sensors and Actuators A, 25-27 (1991) 323-330

[4] G.M. Sessler, J.E. West and R.A. Kubli, Unidirectional, second-order gradient microphone, Journal of Acoustical Society of America, 86, 6 (Dec. 1989) 2063-2066

[5] G.M. Sessler, Second-order gradient unidirectional microphone utilizing an electret transducer, Journal of Acoustical Society of America, 58, 1 (July 1975) 273-278

[6] J.V. Berghe, An adaptive noise canceller for hearing aids using two nearby microphones, Journal of Acoustical Society of America, 103, 6 (June 1998) 3621-3626

[7] Miles, R. N., Robert, R., and Hoy, R. R. [1995] "Mechanically coupled ears for directional hearing in the parasitoid fly *Ormia ochracea*." *Journal of the Acoustical Society of America* 98 (6) 3059-3070.

[8] Miles, R. N., Tieu, T. D., Robert, D. and Hoy, R. R. [1997] "A mechanical analysis of the novel ear of the parasitoid fly *Ormia ochracea*." *Proceedings: Diversity in Auditory Mechanics*. World Scientific, Singapore.

[9] Robert, R., Miles, R. N., and Hoy, R. R. [1996] "Directional hearing by mechanical coupling in the parasitoid fly *Ormia ochracea*," *Journal of Comparative Physiology* **98** (6) 3059-3070.

[10] Robert, D., Miles, R. N. and Hoy, R. R. [1999] "Tympanal hearing in the sarcophagid parasitoid fly *Emblemasoma sp*.: the biomechanics of directional hearing." *The Journal of Experimental Biology* **202** 1865-1876.

[11] Gerzon, MA (1994) Applications of Blumlein shuffling to stereo microphone techniques. J Audio Eng Soc 42:435-453.

[12] K. Petersen, Silicon as a Mechanical Material, Proceedings of IEEE, 70, 5 (May 1982) 420-457

[13] P. Bergveld, The merit of using silicon for the development of hearing aid microphones and intraocular pressure sensors, Sensors and Actuators A, 41-42 (1994) 223-229

[14] H. Yan and E. Kim, Corrugated Diaphragm for Piezoelectric Microphone, IEEE Conference on Emerging Technologies and Factory Automation, (1996) 503-506

[15] V.L. Spiering, S. Bouwstra and J.H.J. Fluitman, Realization of mechanical decoupling zones for package-stress reduction, Sensors and Actuators A, 37-38 (1993) 800-804

[16] J.H. Jerman, The Fabrication and Use of Micromachined Corrugated Silicon Diaphragms, Sensors and Actuators, A21-A23 (1990) 988-992

[17] D. Lapadatu, A. Pyka, J, Dziuban and R. Puers, Corrugated silicon nitride membranes as suspensions in micromachined silicon accelerometers, Journal of Micromechanics and Microengineering, 6, 1 (1996) 73-76

[18] P. Scheeper, W. Olthuis and P. Bergveld, The Design, Fabrication, and Testing of Corrugated Silicon Nitride Diaphragms, Journal of Microelectromechanical Systems, 3,1 (March 1994) 36-42

[19] X. Ding, Behavior and Application of Silicon Diaphragms with a Boss and Corrugations, IEEE Solid-State Sensor and Actuator Workshop (1992) 166-169

[20] A. Zuckerwar, Principles of Operation of Condenser Microphones, AIP Handbook of Condenser Microphones, G. Wong and T. Embleton eds. (1995)

[21] Q. Zou, Z. Tan, Z. Wang, J. Pang, X. Qian, Q. Zhang, R. Lin, S. Yi, H. Gong, L Liu and Z. Li, A Novel Integrated Silicon Capacitive Microphone-Floating Electrode "Electret" Microphone (FEEM), Journal of Microelectromechanical Systems, 7, 2 (June 1998)

[22] Q. Zou, Z. Li and L Liu, Theoretical and experimental studies of single-chip-processed miniature silicon condenser microphone with corrugated diaphragm, Sensors and Actuators A, 63 (1997) 209-215

[23] Y. Zhang and K.D. Wise, Performance of Non-Planar Silicon Diaphragms under Large Deflections, Journal of Microelectromechanical Systems, 3, 2 (June 1994) 59-68

[24] T.B. Gabrielson, Mechanical-Thermal Noise in Micromachined Acoustic and Vibration Sensors, IEEE Transactions on Electron Devices, 40, 5 (May 1993) 903-909

[25] D. Sperring, On Silicon Microphones and Earphones for Hearing Aids, Sensors and Actuators, 18 (1989) 33-44

[26] G.M. Sessler and J.E. West, Directional Transducers, IEEE Transactions on Audio and Electroacoustics, au-19, 1 (March 1971) 19-23

[27] L.L. Beranek, Acoustics, Acoustical Society of America, Woodbury, New York (1993)

[28] G. Popelka and D. Mason, Factors which Affect Measures of Speech Audibility with Hearing Aids, Ear and Hearing, 8, 5 (1987) 109S-118S

[29] C. Pavlovic, Articulation Index Predictions of Speech Intelligibility in Hearing Aid Selection, ASHA, (June/July 1988) 63-65

[30] H. Mueller and M. Killion, An Easy Method For Calculating the Articulation Index, The Hearing Journal, 43, 9 (Sept. 1990) 14-17